

Synthesis, Characterisation, Pharmacological Studies and Quantum Chemical Calculations of Osmium (III) Complex

Sathya Priyadarshini G, Namitha R, Mageswari D and Selvi G*

Department of Chemistry, PSGR Krishnammal College for Women, Coimbatore, Tamilnadu, India

*Corresponding author: Selvi G, Department of Chemistry, PSGR Krishnammal College for Women, Coimbatore, Tamilnadu, India, Tel: 9965152039; E-mail: selvi_gv@rediffmail.com

Received: May 26, 2017; Accepted: July 07, 2017; Published: July 12, 2017

Abstract

New osmium complexes of 4-methyl-2-(salicylidenehydrazino) quinoline H_2L_1 and 4, 6-dimethyl-2-(salicylidenehydrazino) quinoline H_2L_2 were synthesised and characterised by spectroscopic method and TGA analysis. Quantum chemical calculations of ligand was performed using the DFT B3LYP method in the 6-31G (d, p) basis. The calculated results are well agreement with the experimental data. The calculated HOMO and LUMO energies show the chemical activity of the molecule. Nonlinear optical behavior of the ligand was analyzed by using first hyperpolarizability. The calculated first hyperpolarisability shows that the ligand is an attractive molecule for future application in nonlinear optics. Based on the theoretical and spectroscopic studies, it has been confirmed that the ligands H_2L_1 and H_2L_2 coordinated through phenolate oxygen, 'N' of quinoline ring and NH group of hydrazine moiety towards the osmium (III) ion exhibiting octahedral geometry. Antimicrobial result suggests that the complexes having good antimicrobial activity.

Keywords: Ligand; Quinoline; Osmium complex; Drugs

Introduction

Metal complexes with biologically active ligands have attracted more interest from researchers over the last few years. By complexation of these ligands to metal ions, physical and biological activity invitro could be altered significantly [1]. Ligand selection is always an important asset during the design and synthesis of metal complexes. The Chemistry of hydrazinoquinoline derivatives occupy special place because, these ligands developed due to their diverse chelating capability, structural flexibility [2] and pharmacological activities like antibacterial, antifungal, anti-tumoural, antiviral, antimalarial, antituberculosis [3-5]. The use of substituted quinolines are prominent building blocks in both organic and inorganic molecular chemistry with their π -stacking ability and coordination properties. A series of compounds derived from 8-hydroxylquinoline as potential HIV 1 integrase inhibitors were synthesized recently. These compounds show a significant similarity to some novel anti-fungal agents, homoallylamines which possess potent antifungal activity. Another interesting

expedition of quinoline derivatives have good nonlinear properties and have been extensively studied due to their great application in the field of organic light emitting diode (OLED). Quinolines have good electron mobility, good thermal and oxidative stability, high photoluminescence efficiency and good film forming properties which is important for they are used in OLED's [6].

Ruthenium and Osmium-based compounds offer lower toxicity compared to other metals and show different mechanisms of action as well as different spectra of activity compared to Platinum-based drugs [7]. The osmium (III) complexes, particularly the azole chelate ligand, have been widely used in antiproliferative activity [8]. These complexes with pincer ligands have reported as promising alternative to the metal catalyst and are useful due to their photophysical application [9].

The osmium (III) complex has the ability to promote CH activation as well as to accommodate tridentate ligands [10]. The importance of osmium complexes and richness of the quinolines chemistry have now prompted us to explore the reactivity $\text{OsCl}_3 \cdot 3\text{H}_2\text{O}$ towards substituted quinolines, which is suited for NNO coordination mode.

In our present work, new tridentate Schiff bases have been synthesized by condensing 4-methyl-2-hydrazinoquinoline and 4,6-dimethyl-2-hydrazinoquinoline with salicylaldehyde. The 1:1 metal complexes were obtained as a result of interaction of ligand and the metal ion Os (III). The IR and NMR spectra of the ligand are reported both theoretically and experimentally. Also, the thermal analysis, Mulliken charge analysis, FMO analysis and first hyperpolarizability is also reported. All the synthesized complexes have been screened for their *in vitro* biological activities.

Materials and Instruments

Thin layer chromatography (TLC) was performed using glass plates coated with silica gel. Petroleum ether and ethyl acetate was used as eluent. Spots were visualized with iodine. Purification of crude sample was carried out using chromatographic column packed with silica gel. IR spectra were recorded in NICOLET IR 200 FT-IR spectrometer using KBr disc and the absorption frequencies quoted in reciprocal centimeters. UV spectra were recorded in UV-VIS spectrophotometer 3000+, LAB INDIA. ^1H NMR spectra were recorded in AMX (300 MHz) spectrometer using tetra methyl silane (TMS) as internal reference.

The chemical shift was expressed in parts per million (ppm). TGA-DSC curves were recorded on Shimadzu 60 H model using $10^\circ\text{C}/\text{min}$. heating rate. The solvents and reagents used for synthesis were of reagents grade and purified by standard methods.

Preparation of Ligand

Preparation of 4-methyl-2-(salicylidenehydrazino) quinoline (3a) (H_2L_1)

1 mL (6 mmol) of salicylaldehyde (1) was added to 1 g of 4-methyl-2-hydrazinoquinoline (2a) (6 mmol) was dissolved in alcohol. It was refluxed for about 6 h. Completion of the reaction was monitored by TLC. The product was filtered, washed thoroughly with ethanol and dried over vacuum. The compound was recrystallized from ethanol. IR value of ligand ν in cm^{-1} : 3369 (-OH), 3224 (-NH), 1623 (-C=N) and 1251 (-CO). ^1H NMR value of ligand δ in ppm (300 MHz): 9.01(s, 1H), 6.8 (s, 1H), 7.7-6.9 (m, 8H), 3.4 (s, 1H), 2.4 (s, 3H) Yield-65%, M.P- 195°C .

Preparation of 4, 6-dimethyl-2-(salicylidenehydrazino) quinoline (3b) (H₂L₂)

1 mL (6 mmol) of salicylaldehyde (1) was added to 1.12 g of 4, 6-dimethyl-2-hydrazinoquinoline (2b) (6 mmol) was dissolved in alcohol. It was refluxed for about 6 h. Completion of the reaction was monitored by TLC. The product was filtered, washed thoroughly with ethanol and dried under vacuum. The compound was recrystallized from ethanol. IR value of ligand ν in cm⁻¹: 3289 (-OH), 3050 (-NH), 1608 (-C=N) and 1253 (-CO). ¹H NMR value of ligand δ in ppm (300 MHz): 9.0 (s, 1H), 6.7 (s, 1H), 7.68-6.98 (m, 8H), 3.4 (s, 1H), 2.4 (s, 3H), 1.2 (s, 3H) Yield – 72%, M.P-205°C.

Preparation of New Osmium (III) Complex [Os (L) Cl (H₂O)₂]

Preparation of complex A [Os (L₁) Cl (H₂O)₂]

40 mg (0.11 mmol) of osmium trichloridetrihydrate (OsCl₃.3H₂O) in 20 mL of ethanol was added 30 mg (0.11 mmol) of 4-methyl-2-(salicylidenehydrazino) quinoline (H₂L₁). The reaction mixture was kept for continuous stirring about 8 h and completion of the reaction was monitored with TLC. After the completion of the reaction, the reaction mixture was allowed to stand overnight. Dark violet crystals separated, washed with ethanol and dried under vacuum. IR value of complexes ν in cm⁻¹: 3361 (-OH, bs), 1628 (-C=N) and 1050 (-CO). ¹H NMR value of complex δ in ppm (300 MHz): 5.4 (bs, 1H), 7.68-7.75 (m, 8H), 3.4 (s, 1H), 2.4 (s, 3H). Yield-75%, Melting point: >300°C.

Preparation of complex B [Os (L₂) Cl (H₂O)₂]

40 mg (0.11 moles) of osmium trichloridetrihydrate (OsCl₃.3H₂O) in 20 mL of ethanol was added 30 mg (0.11 mmoles) of 4,6-dimethyl-2-(salicylidenehydrazino) quinoline (H₂L₂). The reaction mixture was kept for continuous stirring about 8 h and completion of the reaction was monitored with TLC. After the completion of the reaction, the reaction mixture was allowed to stand overnight. Dark blue crystals separated, washed with ethanol and dried under vacuum. IR value of complexes ν in cm⁻¹: 3398 (-OH, bs), 1607(-C=N) and 1201 (-CO). ¹H NMR value of complex δ in ppm (300 MHz): 5.4 (bs, 1H), 7.68-7.75 (m, 8H), 3.4 (s, 1H), 2.4 (s, 3H), 1.5 (s, 3H). Yield: 75%, Melting point: >300°C.

Antimicrobial activity

The Antibacterial and antifungal activities of Schiff base ligands and complex A and B were studied against the bacteria, *Staphylococcus aureus* (Sa), *Bacillus cereus* (Bc), *Micrococcus luteus* (Ml) and *Escherichia coli* (Ec) and the fungi, *Candida albicans*, *Aspergillus flavus* and *Fusarium sp.* by Well diffusion method.

Each bacterial strain was suspended in nutrient broth; each fungal strain was suspended in potato dextrose broth and incubated at 37°C. Nutrient Agar (NA) plates were seeded with 8 h broth culture of different bacteria. A 16 h broth culture of *Candida albicans*, *Aspergillus flavus* and *Fusarium sp* was used to seed potato dextrose agar (PDA) plates. In each of these plates, wells were cut out using sterile cork borer. Using sterilized dropping pipettes, different concentrations (25%, 50%, 75% and 100%) of samples were carefully added into the wells and allowed to diffuse at room temperature for 2 h. The plates were then incubated at 37°C for 18 h-24 h. *Gentamycin* (10 µg) and *Clotrimazole* (10 µg) were used as positive controls and the respective solvents as negative control. The antimicrobial activity was evaluated by measuring the diameter of inhibition zone.

Quantum chemical calculations

All geometrical optimizations and frequency calculations of the ligand H_2L_1 were done using the Gaussian 09 program. Density functional theory with the Becke three parameters hybrid functional (DFT-B3LYP) calculations were performed with a 6-31G (d, p) basis set. With the aim to arrive at deeper insight of osmium (III) ion interaction with N, N, O coordination environment, the total energy calculation within the DFT framework were carried out.

Results and Discussion

The present work is focused on the study of coordination behavior of hydrazone Schiff bases (viz.) 4-methyl-2-(salicylidinehydrazino) quinoline and 4,6-dimethyl-2-(salicylidinehydrazino) quinoline with $OsCl_3 \cdot 6H_2O$ by using theoretical and experimental results. All the metal complexes and the ligands were prepared by the molar ratio M: L-1: 1. The complexes are intensively coloured stable solids. The ligand and complexes were soluble in ethanol, chloroform, DMSO and DMF. The structures of the synthesized ligands and the complexes were established from their experimental results (i-e) UV, IR, NMR and TGA analysis and are compared with their theoretical results such as IR and NMR of the ligand, Mulliken charge analysis and FMO study. The formation of the metal complexes can be represented by the following equation and SCHEME 1.

Spectroscopic Studies

Electronic spectra

Solution spectral data of the ligands and Os (III) complexes are collected in TABLE 1.

TABLE 1. Analytical and physical data of the ligands and the complexes.

Compounds	Molecular weight (g mol ⁻¹)	Colour	λ in nm	Molar conductance (mho cm ² mol ⁻¹)
L_1H_2	277.01	White	261, 287, 387	-
L_2H_2	292.03	Yellow	246, 290, 325	-
$[Os (H_2O)_2 (Cl) L_1] \cdot H_2O$	536.96	Violet	575, 405, 205	9
$[Os (H_2O)_2 (Cl) L_2] \cdot H_2O$	550.99	blue	560, 400, 246	14

The free ligand H_2L_1 showed three absorption bands at 261 nm, 287 nm and 387 nm. The first band would be assigned to $\pi-\pi^*$ transition within the aromatic rings. The second band would be due to $n-\pi^*$ transition within 'C=N' group. The absorption band at 387 nm is due to charge transfer transition [11,12]. Complex A showed three absorption bands at 575 nm, 405 nm and 205 nm. The band at 575 nm is due to d-d transition.

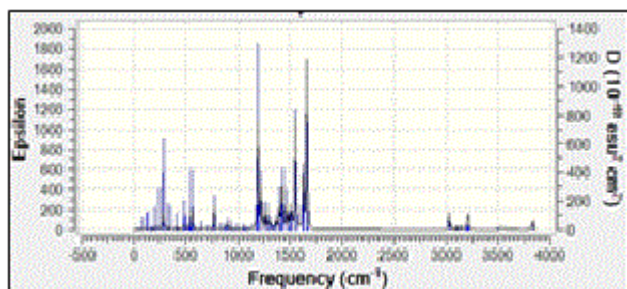


FIG. 1. Theoretical IR spectrum of ligand L_1H_2 .

IR spectra

The IR spectra data of the Schiff base ligands (L_1H_2) (experimentally and theoretically); L_2H_2 and their complexes are presented in the TABLE 2 and FIG. 2 and 3 of IR spectra of ligand and complexes. IR spectra of the Schiff base ligand (L_1H_2) and L_2H_2 exhibited a strong peak at 1623 cm^{-1} and 1608 cm^{-1} was assigned to azomethine group, and for $-OH$, $-NH$, C-O stretching vibrations were observed at 3369 cm^{-1} , 3224 cm^{-1} and 1251 cm^{-1} . IR Spectra of the complex A showed a characteristic peak at 1628 cm^{-1} and 1050 cm^{-1} due to stretching vibrations of $-C=N$ and $-C=O$ groups [13].

TABLE 2. Characteristic IR bands of the ligand and the complexes (in cm^{-1}).

Compounds	$\nu(\text{O-H})$	$\nu(\text{N-H})$	$\nu(\text{C=N})$ azomethine	$\nu(\text{C-O})$
L_1H_2	3369	3224	1623	1251
L_2H_2	3289	3050	1608	1253
L_2H_2 (theoretical)	3498	3213	1658	1192
$[\text{Os}(\text{H}_2\text{O})_2(\text{Cl})L_1] \cdot \text{H}_2\text{O}$	3361(bs)	-	1628	1050
$[\text{Os}(\text{H}_2\text{O})_2(\text{Cl})L_2] \cdot \text{H}_2\text{O}$	3398(bs)	-	1607	1201

The Schiff base ligand has four potential donor sites (i) Quinoline nitrogen (ii) hydrazino nitrogen (iii) azomethine nitrogen (iv) phenolic oxygen. In order to determine the coordination sites, the IR spectra of the complexes were compared with those of the free ligands. Upon comparison, IR value of the metal complex does not show a remarkable shifting frequency of $\nu(\text{C=N})$ compared to its respective ligand, this suggests that the nitrogen atom in azomethine group has not participated in the coordination. The broadened band at 3361 cm^{-1} - 3400 cm^{-1} revealed that the presence of coordinated water molecule in the metal complexes.

In the free ligand, a strong band at 1200 cm^{-1} due the C-O (phenolic) shifts to lower frequency in the complexes indicates the coordination of the phenolic oxygen atom to the metal ion. In addition, the change in the intensity of $-OH$ of the IR region shows the disappearance of $-OH$ and of the hydroxyl and appearance of $-OH$ of H_2O [14]. Theoretical IR spectra of ligand is shown in FIG. 1. The important assignments (cm^{-1}) are 3498, 3213, 1658 and 1192, these values agree with experimental vibrational frequencies and hence prove the reliability of the applied level of theory [15].

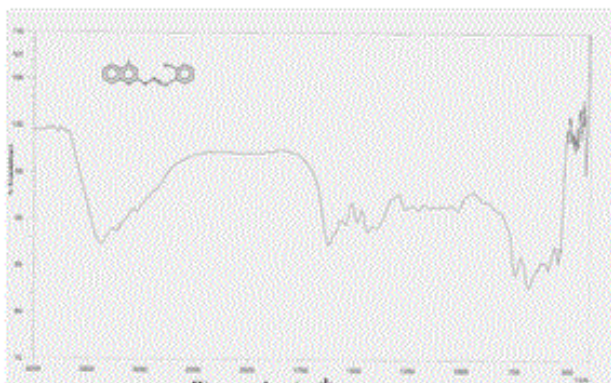


FIG. 2. IR spectrum of ligand L_1H_2 .

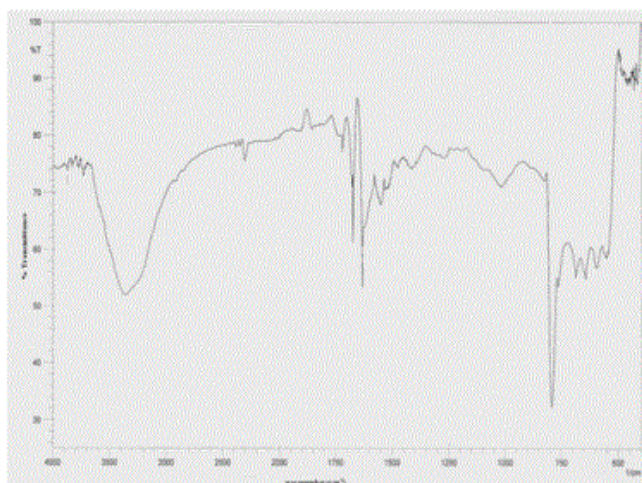


FIG. 3. IR spectrum of complex A.

¹H NMR spectra

The NMR Spectra of the Schiff bases, H₂L₁ (both experimentally and theoretically), H₂L₂ and their Os (III) complexes were recorded in CDCl₃ data are given in TABLE 3 and FIG. 4, 5 and 6. ¹H NMR Spectra (ppm) of the ligand (L₁H₂) showed signals δ 9.01 are assignable for –NH protons, δ 7.7-6.9 for aromatic protons, δ 6.7 for –OH protons, δ 3.4 for azomethine protons and δ 2.4 for methyl protons. ¹H NMR Spectra (ppm) of the complex A showed signals at δ 7.7-6.9 multiplet for aromatic protons, δ 3.4, singlet for azomethine proton and δ 2.4, singlet for methyl proton [15].

The spectra of the complexes are examined in comparison with those of the parent Schiff bases. Upon examination, it was found that –OH and –NH signal that appeared in the spectrum of the H₂L₁ ligand at 9 ppm and 6.8 ppm completely. Disappeared in the spectrum of its Os (III) complex indicating that the –OH and –NH protons are removed by chelation with Os (III) ion¹. The theoretical ¹H NMR data of the meaning full region of the ligand well coincides with experimental outcome [16].

TABLE 3. ¹H-NMR spectral data of the ligand and the Os (III) complexes (in ppm).

Compounds	-NH	-C-OH	Ar-H	-CH=N	-CH ₃	-CH ₃
L ₁ H ₂ (3a)	9.01	6.8	7.7-6.9	3.4	2.4	-
L ₂ H ₂ (3b)	9.0	6.7	7.68-6.9	3.4	2.4	1.2
[Os (H ₂ O) ₂ (Cl) L ₁]. H ₂ O Complex A	-	5.4(bs)	7.68-7.75	3.4	2.4	-
[Os (H ₂ O) ₂ (Cl) L ₂]. H ₂ O Complex B	-	5.4(bs)	7.68-7.75	3.4	2.4	1.5

Molar conductivity measurements

Molar conductivities of the complexes were measured in DMSO solution within the range of 10⁻³ concentrations. Both the complexes show molar conductance in the range of 9-15 mho cm² mol⁻¹ are shown in TABLE 1. These low values indicate the non-electrolytic nature of the complexes [17].

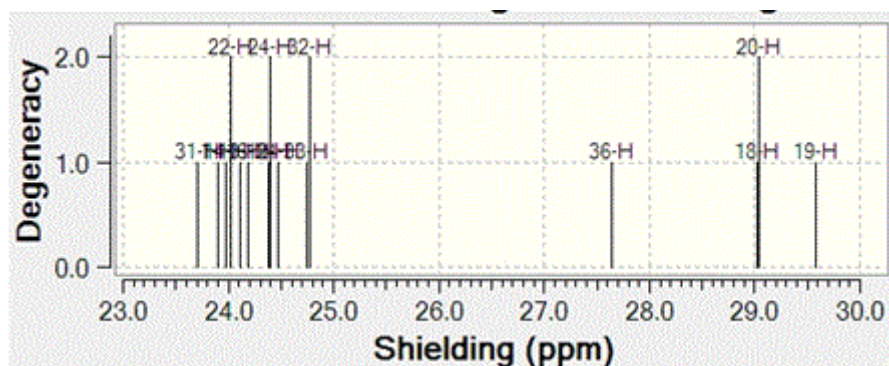


FIG. 4. Theoretical ^1H NMR spectrum of ligand L_1H_2 .

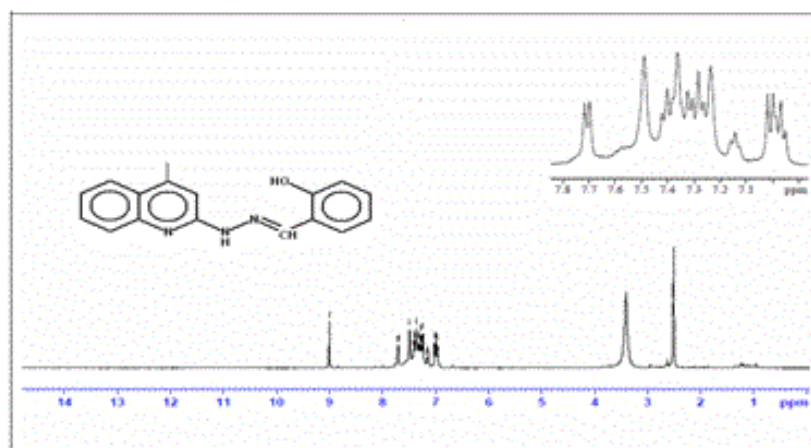


FIG. 5. ^1H NMR spectrum of ligand L_1H_2 .

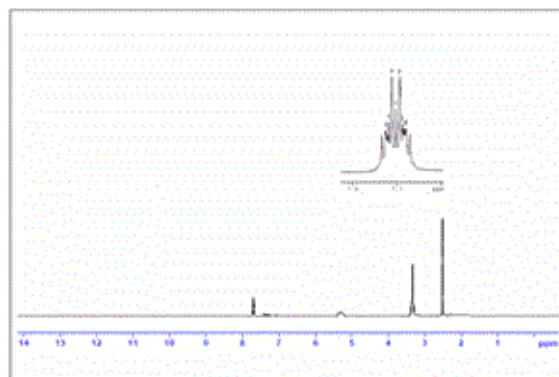


FIG. 6. ^1H NMR spectrum of complex A.

Thermal analysis

The thermogravimetric studies [18] of the complex A FIG. 7 of the present investigation was carried at the heating rate of $10^\circ\text{C min}^{-1}$ under nitrogen atmosphere and weight loss as measured from the ambient temperature up to 1000°C . The results obtained for both ligand L_1H_2 and complex A were tabulated (TABLE 4).

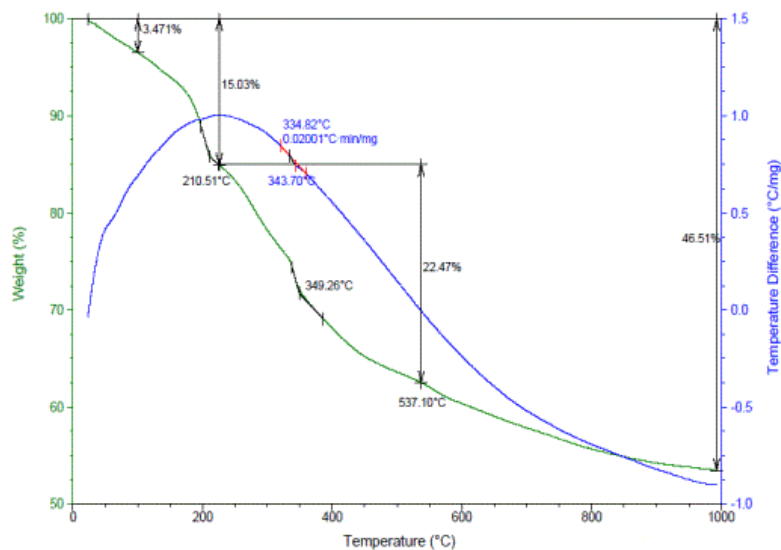


FIG. 7. TGA Curve of the metal complex A.

TGA analysis showed that this ligand decomposed into one step from 193.04°C to 411.16°C. This step corresponds to the complete decomposition of H_2L_1 deduced from mass loss calculation.

The TGA of the metal complex A (FIG. 7) shows three stage decomposition

1. The first decomposition is obtained in the temperature range 110°C. The percentage weight loss (3%) in this range corresponds to the loss of one lattice water molecules.
2. The second stage decomposition is obtained in the temperature range 210.51, (12%) loss indicates the loss of two coordinated water molecules and one chlorine atom.
3. The third stage decomposition is obtained in the temperature range of 400°C-1000°C. The percentage weight loss in the range corresponds to the ligand decomposition and leaving the metal residue.

The residues subsequently fragments of complex A through the several exothermic processes are shown by the DSC curve. (blue color line in FIG. 7).

TABLE 4. TGA data of the ligand H_2L_1 and the complex A.

Compounds	Decomposition temperature	Weight loss (%) observed	Cal/ found	Assignments
H_2L_1 (3a)	193°C-411.6°C	-	-	Complete decomposition of ligand in one step
[Os (H_2O) ₂ L ₁ (Cl)]. H_2O	110°C	3.47	3%	Loss of water molecule in the lattice
	210°C	12.03	12%	Loss of coordinated one molecule of water and two chlorine atoms
	537°C	22.47	22%	Loss due to the remaining organic moiety

Mulliken charge analysis

The atomic population and charge distribution in the molecule obtained by the Mulliken analysis and this distribution of the ligand has been calculated by using DFT/B3LYP/6-31G (d, p) level theory [19]. The optimized geometry of the ligand H₂L₁ was obtained and shown in FIG. 8.

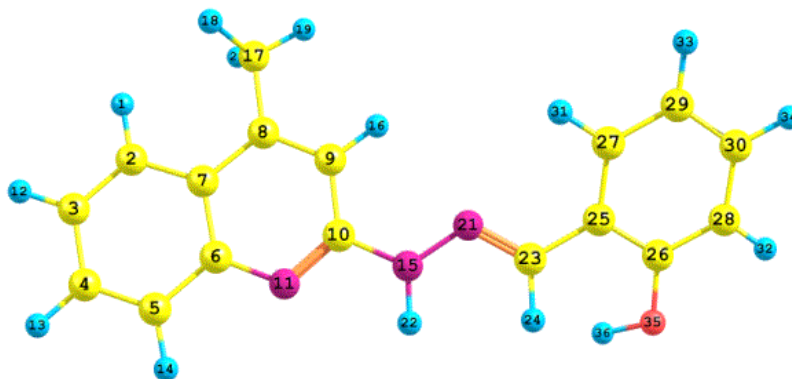


FIG. 8. Optimized geometry of ligand.

The atomic charges of carbon vary within the range of +0.5277 to -0.1406. From the mulliken charges, it is predicted that the atom N-11(-0.6203) O-35((-0. 5618) and N-15 (-0.4273) acts as a donor site whereas N-21 (-0.2358) is less active towards the coordination.

Frontier molecular orbital analysis

Frontier molecular orbital plays a vital role in the electrical and optical properties as well as chemical reactions. According to FMO of chemical reactivity, transition of electron is due to interactions with other species.

TABLE 5. FMO analysis of ligand H₂L₁.

Molecular property	B3LYP/6-31G (d, p)
E _{HOMO}	-5.3041 eV
E _{LUMO}	-1.4150 eV
Energy gap	3.8891 eV

The frontier energy gap of the ligand H₂L₁ (TABLE 5) is found to be 3.8891eV. The small HOMO-LUMO gap automatically means low excitation energy for the excited states, low stability and highly reactive. The frontier orbitals of the ligand H₂ L₁ (FIG. 9 and 10).

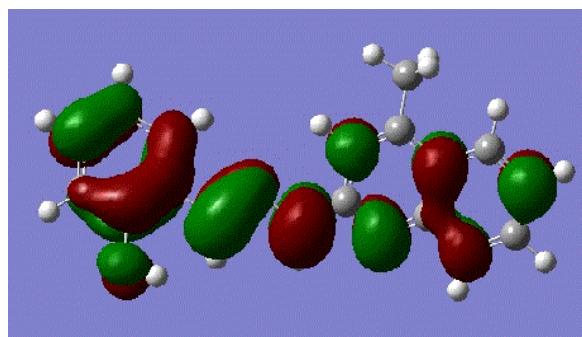


FIG. 9. HOMO.

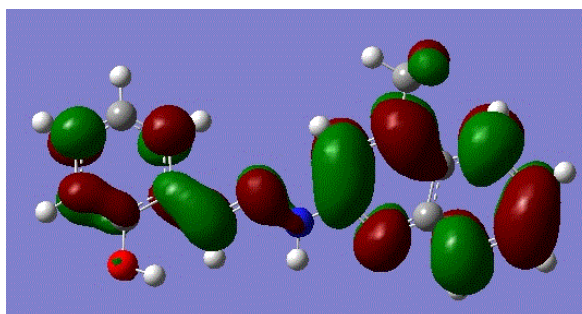


FIG. 10. LUMO energy gap=3.8891eV.

The larger the energy gap, the harder the molecule. The hardness has been associated with the stability of the chemical system. The electron affinity and the global electrophilicity index is also calculated and tabulated in TABLE 6.

TABLE 6. Quantum chemical parameters of the ligand H₂L₁.

Total Energy after 15 cycles	-896.335722804 A.U.
Ionization energy	5.3041 eV
Electron affinity A	1.4150 eV
The global hardness	1.9445 eV
Electronic chemical potential	3.3565 eV
The global electrophilicity index	2.8969
Dipole moment	1.1825

Non-linear optical effects

Nonlinear optics deals with the interaction of applied electromagnetic fields in various materials to generate new electromagnetic fields, altered in wavenumber, phase or other physical properties. The calculated first hyperpolarisability of the ligand is 0.427×10^{-30} e.s.u which is four times that of standard NLO material urea.

Pharmacological activities

The results of inhibition zone in mm of ligand, complexes A and B for antibacterial and antifungal activity shown in TABLE 7. The histogram of antimicrobial activity was shown in FIG. 11. The antibacterial activity of the ligand, complexes A and B against the bacteria namely *Staphylococcus aureus* (Sa), *Micrococcus luteus* (Ml), *Bacillus cereus* (Bc), *Escherichia coli*. It was found that the complex was active against *Staphylococcus aureus*, is almost equal to the standard gentamycin. The complex was less active against *Bacillus cereus* and *Escherichia coli* when compared to the standard.

TABLE 7. Antimicrobial activity of the metal complexes (inhibition zone value in mm).

Compound	Bc	Ml	Ec	Sa	Ca	Af
[Os (H ₂ O) ₂ (L ₁) (Cl)]. H ₂ O. Complex A	12	11	10	13	12	8
[Os (H ₂ O) ₂ (L ₂) (Cl)]. H ₂ O. Complex B	10	11	6	11	11	8
Gentamycin	15	13	13	16		
Clotrimazole					17	21

The enhancement in the activity may be rationalized on the basis that ligands mainly possess C=N bond. The enhanced activity of the complexes over the ligand can be explained on the basis of chelation theory [20]. It is observed that, in a complex, the positive charge of metal is partially shared with the donor atoms present in the ligand and there may be pi electron delocalization over the whole chelation. The increase in the lipophilic character of the metal chelate and favors its permeation through the lipid layer of the bacterial membranes. The heterocyclic Schiff bases with different fungal groups have greater tendency to interact with nucleoside bases even after complexation with metal ions present in the biosystem can act as promising bactericides because they always tend to interact with enzymatic functional groups, in order to achieve higher coordination number. There are also some other factors which increase the activity namely solubility, conductivity and bond length between the metal and ligand [21].

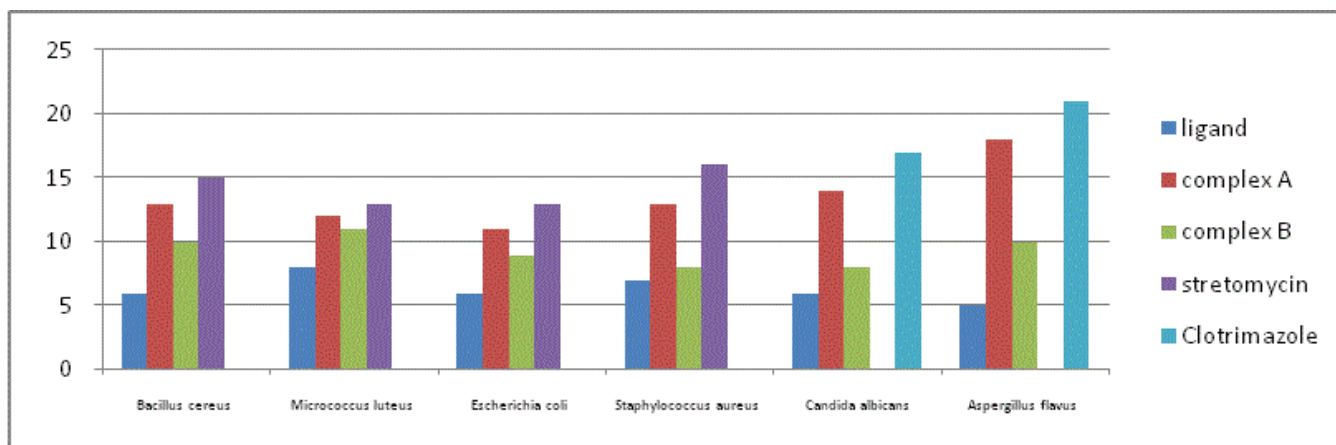


FIG. 11. Histograms of antimicrobial activity.

Conclusion

Osmium complexes having hydrazino quinolines ligands were synthesized from $[\text{OsCl}_3 \cdot 3\text{H}_2\text{O}]$ with 4-methyl-2-(salicylidenehydrazino) quinoline (H_2L_1) and 4, 6-dimethyl-2-(salicylidenehydrazino) quinoline (H_2L_2). The targeted compound was confirmed by UV, IR, ^1H NMR spectra, thermal studies and theoretical studies. The theoretical results indicate that mode of co-ordination of the ligand to the metal is N-15, N-21 and O-35. The hydrazino quinoline Schiff bases are tridentate and the mode of coordination through NNO (i.e.) phenolate oxygen, nitrogen atom of quinoline and nitrogen atom of hydrazine moiety and suggested geometry as octahedral complexes. From this we conclude that the experimental results of the complex formed is coincide with theoretical result. The synthesized complexes were screened for antibacterial and antifungal activity. The complexes exhibited good antimicrobial activity. The theoretical prediction supports that N-15, N-11 and O-35 of the ligand are involved in the coordination with the metal ion.

REFERENCES

1. Filak LK, Goschl S, Heffler P. Ruthenium and osmium-arene complexes of 2-substituted Indolo [3, 2-c] quinolines: Synthesis, structure, spectroscopic properties, and antiproliferative activity. *Organometallics*. 2010;32:903-83.
2. Rao S, Mishra DD. Oxovanadium binuclear (IV) Schiff base complexes derived from aroyl hydrazones having subnormal magnetic moments. *Polyhedron*. 1997;16:1825-9.
3. West DX, Liberta AE. Thiosemicarbazone complexes of copper(II): Structural and biological studies. *Coord Chem Rev*. 1993;123:49-71.
4. Srivastava A, Chandra A, Singh A. Thiophene-fused quinoline analogues: Facile synthesis of 3-amino-2-cyanothieno [2, 3-b] quinolines from 2-chloro-3-cyanoquinolines. *Indian J of Chem*. 2005;44:2077.
5. Dubey PL, Srinivas Rao S, Aparna V. Synthesis of some novel 3-(2-chloro-3-quinolyl)-5-phenyl [1, 3] thiazolo [2, 3-c] [1, 2, 4] triazoles. *Heterocyclic communications*. 2003;9:281-6.
6. Fazal E, Yohannan Panicker C, Tresavarghese H, et al. Spectroscopic investigation (FT-IR, FT-Raman), HOMO–LUMO. NBO analysis and molecular docking study of 4-chlorophenyl quinoline-2-carboxylate. *Spectrochimica Acta Part A*. 2015;145:260-9.
7. Novak MS, Büchel GE, Keppler BK, et al. Biological properties of novel ruthenium- and osmium-nitrosyl complexes with azole heterocycles. *J Biol Inorg Chem*. 2016;21:347-56.
8. Stepaneko IN. Synthesis, structure, spectroscopic properties, and antiproliferative activity *in vitro* of novel osmium (III) complexes with azole heterocycles. *J of Inorg Chem*. 2008;47:7338-47.
9. Asensio G, Cuenca A, Vlencia M. Osmium (III) complexes with POP pincer ligands: Preparation from commercially available $\text{OsCl}_3 \cdot 3\text{H}_2\text{O}$ and their X-ray structures. *J of Inorg Chem*. 2010;49:8665-7.
10. Judith A, Howard K, Sparkes HA, et al. Osmium assisted C–H activation and C double bond; length as m–N cleavage of N-(2'-hydroxyphenyl) benzaldimines. Synthesis, structure and electrochemical properties of some organoosmium complexes. *J of Organometallic Chem*. 695:2068.
11. Mounika K, Anupama B. Synthesis, characterization and biological activity of a Schiff base derived from 3-ethoxy salicylaldehyde and 2-amino benzoic acid and its transition metal complexes. *J of Scientific Res*. 2010;2:513.
12. Abdou S. Synthesis and characterization of chromium (III), molybdenum (III), ruthenium (III) and osmium (III) complexes with N_2O_2 -Schiff bases of 2-hydroxy-1-naphthaldimines. *Trans Met Chem*. 2004;29:543-9.

13. Schmid WF. Highly antiproliferative ruthenium (II) and osmium (II) arene complexes with paullone-derived ligands. *Organometallics*. 2007;26:6643-52.
14. Rajeev TU, Yohannan PC, Hema T, et al. Spectroscopic (FT-IR, FT-Raman) investigations and quantum chemical calculations of 4-hydroxy-2-oxo-1, 2-dihydroquinoline-7-carboxylic acid. *Spectrochimica Acta Part A*. 2014;121:404-14.
15. Kurdekar GS. Synthesis, characterization, antibiogram and DNA binding studies of novel Co (II), Ni (II), Cu (II), and Zn (II) complexes of Schiff base ligands with quinoline core. *Med Chem Res*. 2011;20:421-9.
16. Subramanian N, Sudaraganesan N, Sudha S, et al. Experimental and theoretical investigation of the molecular and electronic structure of anticancer drug camptothecin. *Spectrochimica Acta Part A*. 2011;8:1058-67.
17. Xi PX, Xu ZH. Study on synthesis, structure, and DNA-binding of Ni, Zn complexes with 2-phenylquinoline-4-carboylhydrazide. *J of Inorg Biochem*. 2009;103:210-8.
18. Muhammed GG, Omar MM. Metal complexes of Schiff bases, preparation, characterization and biological activity. *Turkish J of Chem*. 2006;30:361-82.
19. Suliman FO, Al-Nafai I, Al-Busafi SN. Synthesis, characterization and DFT calculation of 4-fluorophenyl substituted tris (8- hydroxyquinoline) aluminum (III) complexes. *Spectrochimica Acta Part A*. 2014;118:66-72.
20. Karekel MR, Biradar V. Synthesis, characterization, antimicrobial, DNA cleavage, and antioxidant studies of some metal complexes derived from Schiff base containing indole and quinoline moieties. *J of Bioinorg Chem and App*. 2013;2013:1-16.
21. Sharma AK, Chandra S. Complexation of nitrogen and sulphur donor Schiff's base ligand to Cr (III) and Ni (II) metal ions: Synthesis, spectroscopic and antipathogenic studies. *Spectrochimica Acta Part A*. 2011;78:337-42.